



Nitrate removal by using chitosan/zeolite molecular sieves composite at low temperature: characterization, mechanism, and regeneration studies

Yunan Gao^{a,*}, Shunyu Bao^a, Li Zhang^a, Lunqiu Zhang^b

^aSchool of Municipal and Environmental Engineering, Shenyang Jianzhu University, Shenyang 110168, China,

Tel. +86 15998380991; emails: gaoyunan01@163.com (Y. Gao), 2426901526@qq.com (S. Bao), 77377200@qq.com (L. Zhang)

^bCollege of Petroleum Engineering, Liaoning Shihua University, Fushun 113000, China, email: 105520722@qq.com (L. Zhang)

Received 30 October 2019; Accepted 6 June 2020

ABSTRACT

In this manuscript, a chitosan cross-linked zeolite molecular sieve (CTS/ZMS) was prepared and studied as adsorbent for nitrate ion from the ground water having low temperature below 10°C. Batch equilibration studies indicated that the prepared CTS/ZMS composite had good adsorption capacity (2.11 mg/g) from neutral water (pH = 7.0) under low temperature (9°C ± 1°C) which make it suitable for treatment of drinking water at low temperature. In batch equilibration method, 1.0 g of CTS/ZMS composite was able to remove 70.2% of nitrate ion from 100 mL of water containing 30 mg/L of nitrate ions and having a neutral pH of 7 when contacted for 420 min at a temperature of 9°C ± 1°C. Thermodynamic studies showed that the adsorption of nitrates was spontaneous, endothermic, and thermodynamically favourable. The kinetic studies indicated that the pseudo-second-order model fit the experimental data well ($R^2 = 0.989$), and it was also observed that adsorption isotherms can be well-described by Langmuir models ($R^2 = 0.989$). The physicochemical characteristics of the CTS/ZMS composites before and after the nitrate adsorption were demonstrated by Fourier-transform infrared spectroscopy, X-ray diffraction, and X-ray photoelectron spectroscopy methods. When the solution pH value was lower than the $pH_{PZC} = 10.0$, the surface active groups of the CTS/ZMS composites like -OH and -NH₂ were positively charged (OH₂⁺, NH₃⁺). Therefore, electrostatic attraction between NO₃⁻ and OH₂⁺ and/or NH₃⁺ led to the removal of nitrate from the contaminated water. Regeneration experiments showed the CTS/ZMS composites could be reused at least five times without any considerable loss of adsorption capacity by treating with Na₂CO₃.

Keywords: Nitrate; Adsorption; Zeolite molecular sieves; Chitosan; Regeneration

1. Introduction

Pollution of ground water from nitrate ions is a major environmental concern all over the world, especially in China. Nitrates are major constituents of agricultural fertilizers as they have high solubility and nutritional value towards aquatic plants [1]. During rainfall, penetration of nitrate takes place through the soil elements with subsequent leakage into the ground water. In the north-eastern parts of China, the source of drinking water is mainly from the ground water. However, China's State of the Environment

Bulletin pointed out that among 2,833 groundwater testing sites, the water in 46.9% of the monitored sites were polluted due to nitrate [2]. Higher level of nitrate concentration in drinking water may lead to various health complications including eutrophication and infectious diseases, such as cyanosis and cancer of the alimentary canal [3,4]. In 2016, the limiting concentration of nitrate ion in the drinking water was reduced from 20 to 10 mg/L by China's Standard of Drinking Water Quality (GB5749-2006) [5]. Therefore, nitrate removal has become considerably important from the perspective of human health and environment.

* Corresponding author.

Water purification plants in China generally use conventional treatment processes such as coagulation–sedimentation–filtration–disinfection [6]. However, nitrate removal by these methods is inefficient, especially for ground water as it is always under low temperature, below 10°C [7]. Various techniques such as ion-exchange [8], biological denitrification [9], electrochemical reduction [10], chemical reduction [11], and reverse osmosis [12] have been established for nitrate removal from the surface water or waste water stream. However, these developed methods for nitrate removal are not easily scalable for large scale implementation due to certain disadvantages like large expense, generation of additional by-products, and incompetency.

Adsorption method is a widely used technique in water treatment due to simple nature of the process, absence of by-product and recyclable nature [13,14]. Wide varieties of adsorbents such as zeolite-based [15], mineral-based [16], and nanoparticles [17] have been applied for nitrate removal from water at room temperature [18]. However, as these adsorbents have certain inherent limitations including difficult preparation process, higher cost of the nano-materials, strong dependence on the pH values, and reduced efficiency at lower temperature, their practical applications might be limited. As a consequence, development of an easily synthesized, technically feasible, and environmental friendly adsorbent is of prime importance for nitrate removal [19].

Chitosan (CTS) is the product formed via chitin deacetylation and is a white amorphous, translucent, water-insoluble solid. The characteristic structure of chitosan containing hydroxyl(–OH) and amino(–NH₂) groups determines the properties of chitosan [20]. Due to the protonation of the amino group in the acidic solution, it can exhibit the characteristics of a cationic flocculant and thus exhibit the ability for removal of nitrate from the water [21]. However, chitosan is not acid and alkali resistant and has poor mechanical strength and hence require a support for process applications. Zeolite molecular sieve (ZMS) is a kind of synthetic sodium zeolite, having tetrahedral structure with a Si–Al–Si framework and a large specific surface area [22]. ZMS, as a common nanomaterial, has been widely investigated for water purification [23]. Cross linking of chitosan with ZMS (CTS/ZMS) can improve acid alkali resistance and mechanical strength. In addition, the CTS/ZMS is cheaper than the nano-sorbents, simpler to prepare, and is safer to use in the treatment of drinking water due to the non-toxicity of the two materials.

Composite adsorbent materials formed via cross linking of chitosan with different materials have been successfully applied for the removal of nitrate [15,21,24–28]. However, there are few literature reports on the application of adsorbent for nitrate removal from water at lower temperature under 10°C. Arora et al. [15] reported the nitrate removal from cold regions at two different temperatures of 4°C and 20°C using surface modified natural zeolite by chitosan. The authors concluded that there was no apparent change in the nitrate removal rate with change in temperature. Hu et al. [21] studied nitrate removal from the aqueous solution using granular chitosan-Fe(III)–Al(III) complex at 15°C temperature and found that in presence of 150 mg/L nitrate concentration, the adsorption capacity of the complex was

8.58 mg/g. Teimouri et al. [24] investigated a complex of chitosan/zeolite/nano-ZrO₂ for adsorption of nitrate from water which showed a removal rate of 42.5% for nitrate from water at 35°C. However, the best results for Hu et al. [21] and Teimouri et al. [24] were obtained from pH 3.0, and thus were not suitable for the treatment of drinking water.

Hence, chitosan cross-linked zeolite molecular sieve (CTS/ZMS) was investigated for its nitrate removal efficiency from low temperature. In order to study the low temperature nitrate adsorption properties of this adsorbent material, laboratory tests were carried out at 8°C–10°C temperature range. Various parameters affecting the nitrate removal efficiency and adsorption capacity of the sorbent such as adsorbent dosage, contact time, pH value, and temperature were investigated in detail. Fourier transform infrared spectroscopy (FTIR), X-ray diffraction (XRD), and X-ray photoelectron spectroscopy (XPS) were used to characterize the adsorption characteristics of the CTS/ZMS particles. Adsorption kinetics, isotherm, and thermodynamics tests for nitrate sorption were also studied for the CTS/ZMS adsorbent.

2. Experimental procedure

2.1. Material

Chitosan with 90% deacetylated was purchased from Shanghai Sinopharm Group (Shanghai, China). ZMS was purchased from Shanghai New Molecular Sieve Co., Ltd., (Shanghai, China). Potassium nitrate (0.20–0.22 g/L), glutaraldehyde (25 vol.%), hydrochloric acid (HCl, 1 mol/L), acetic acid (4 vol.%), sodium hydroxide (NaOH, 1 mol/L), sodium chloride (NaCl, 1 mol/L), sodium carbonate (Na₂CO₃, 1 mol/L), sodium bicarbonate (NaHCO₃, 1 mol/L), calcium chloride (CaCl₂, 1 mol/L) were supplied by Sinopharm Chemical Reagent Co., Ltd. The purchased chemicals are analytical reagent grade.

2.2. Preparation of sorbent media

CTS/ZMS adsorbent was prepared as following: Chitosan solution (7 g/L) was prepared by adding chitosan in acetic acid solution (4 vol.%), configured as chitosan acetate sol. ZMS was washed with deionized water and heated at 105°C for 2 h, then added to glutaraldehyde (25 vol.%) for 4 h. These particles of ZMSs with glutaraldehyde were then added to chitosan acetate sol, the mass ratio (m/m) of corresponding ZMS to chitosan was 100:7. The composites were stirred at the speed of 130 rpm for 10 h at temperature of 30°C to obtain the sorbent media, then added to distilled water to remove acetic acid and glutaraldehyde, dried in the oven at 60°C for 5 h [29].

2.3. Characterizations

XRD patterns of CTS/ZMS composites were obtained with an X-ray diffractometer (Xpemt, PANalytical, Netherlands). FTIR spectra were obtained on FTIR spectrophotometer (Tensor 27, Burker, Germany) with the scanning range from 4,000 to 400 cm⁻¹. XPS (Thermo Fisher, USA) analyzed the surface chemistry of CTS/ZMS adsorbent

materials before and after adsorption of nitrate with the monochromatic Al K α X-ray radiation. The zero charge point of CTS/ZMS composites was studied by batch equilibrium techniques described by Chutia et al. [30].

2.4. Adsorption experiment

Batch equilibration studies were carried out to investigate the adsorption behavior of the sorbent. Simulated water solution corresponding to 30 mg/L of nitrate concentration corresponding to the contaminated groundwater of Shenyang, Liaoning, China was prepared. The initial and equilibrium concentration of nitrate were determined by an ultraviolet-visible spectrophotometer (752, Shanghai Spectrum Instrument Co., Ltd., China). The water samples were pretreated by a microporous membrane (pore size 0.45 μm) for removal of the particles and impurities from water before the nitrate concentration determination.

Effects of the adsorbent dose and contact time on the nitrate removal of CTS/ZMS adsorbent were studied from water solution containing nitrate concentration of 30 mg/L when the pH and the temperature was $7^\circ\text{C} \pm 0.5^\circ\text{C}$ and $9^\circ\text{C} \pm 1^\circ\text{C}$, respectively.

To study the effect of initial pH on the removal of nitrate by CTS/ZMS, 1.0 g of the adsorbent was contacted with 100 mL aqueous solution containing 30 mg/L of nitrate. The initial pH value was adjusted from 4 to 12 with increment of one unit by 0.1 M HCl or 0.1 M NaOH. Equilibrium pH of each sample was also measured after 420 min.

Effect of temperature on nitrate removal was studied by adding 1.0 g of CTS/ZMS adsorbent in 100 mL of solution at pH 7 containing 30 mg/L nitrate at varying temperatures. Each sample was measured after reaching equilibrium with rotating speed of 130 rpm.

The adsorption capacity (mg/g) and nitrate removal efficiency (%) were calculated as per Eqs. (1) and (2), respectively:

$$q_e = \frac{(C_0 - C_e)V}{m} \quad (1)$$

$$R = \frac{(C_0 - C_e)}{C_0} \times 100\% \quad (2)$$

where q_e is the equilibrium adsorption capacity (mg/g), C_0 is the initial concentration of nitrate (mg/L), C_e is the equilibrium concentration of nitrate (mg/L), m is the mass of the adsorbent (g), V is the volume of the solution (L), R is the nitrate removal efficiency (%) of the CTS/ZMS composite. The analysis results of the tests were the average values of three replicates.

2.5. Thermodynamic experiment

To evaluate the thermodynamic feasibility and confirm the nature of the adsorption process, the three basic thermodynamic parameters, standard Gibbs free energy change (ΔG°), standard enthalpy change (ΔH°), and standard entropy change (ΔS°) were calculated as the following equations [31]:

$$\Delta G^\circ = -RT \ln K = \Delta H^\circ - T\Delta S^\circ \quad (3)$$

$$K = \frac{(C_0 - C_e)}{C_e \times m} = \frac{q_e}{C_e} \quad (4)$$

$$\ln K = \frac{\Delta S^\circ}{R} - \frac{\Delta H^\circ}{RT} \quad (5)$$

where R is the universal gas constant having the value of 8.314 J/(mol K) and T is the absolute temperature (K). q_e is the concentration of the adsorbed nitrate (mg/g) and K is the apparent equilibrium constant.

2.6. Adsorption isotherm experiment

To study the adsorption isotherm, batch experiments were carried out using varying concentration of nitrate at pH 7 and temperature of $9^\circ\text{C} \pm 1^\circ\text{C}$. Different concentrations of nitrate (10–80 mg/L) in 100 mL water samples were treated with 1.0 g CTS/ZMS for contact time of 420 min in a thermostatic shaker. Finally, the suspension was passed through a needle filter (pore size 0.45 μm), and the nitrate concentration was analyzed.

Langmuir [Eq. (6)] and Freundlich [Eq. (7)] isotherms are described by the following equations [32,33]:

$$\frac{C_e}{q_e} = \frac{C_e}{q_m} + \frac{1}{q_m K_L} \quad (6)$$

$$q_e = K_F C_e^{1/n} \quad (7)$$

where, q_e is the amount of adsorption (mg/g) and q_m (mg/g) indicates the maximum adsorption capacity. K_L (L/mg) is the Langmuir isotherm coefficient, $1/n$ is the Freundlich constant representing adsorption capacity, and K_F [(mg/g)/(mg/L) $^{1/n}$] is the Freundlich constant representing the adsorption intensity.

2.7. Adsorption kinetics experiment

To measure the adsorption kinetics of CTS/ZMS, 1.0 g of the sorbent was added to 100 mL of water solution containing 30 mg/L of nitrate and stirred at 130 rpm. Samples were taken after certain time intervals (15, 30, 60, 120, 180, 240, 300, 360, 420, 480, 540, and 600 min) and then nitrate concentration was analyzed.

The data was modeled using Lagergren pseudo-first-order kinetic model [Eq. (8)] and pseudo-second-order kinetic model [Eq. (9)]. A pseudo-first-order model can be represented as [34]:

$$\log(q_e - q_t) = \log q_e - \frac{k_1 t}{2.303} \quad (8)$$

where q_t and q_e are the adsorption amounts of nitrate at time t and at time of equilibrium (mg/g), respectively; k_1 (1/min) is the constant of the quasi-first-order kinetic model. The quasi-second-order kinetic model was based on the assumption that the adsorption rate, is controlled by the chemical adsorption mechanism, the formula is as follows [35]:

$$\frac{t}{q_t} = \frac{1}{k_2 q_e^2} + \frac{t}{q_e} \quad (9)$$

where k_2 is the second-order adsorption rate constant (g/(mg min)).

2.8. Regeneration experiment

2.8.1. Water regeneration

1.0 g of the CTS/ZMS composite saturated with nitrate was placed in 100 mL of distilled water, and stirred at 130 rpm for 24 h in the room temperature. After completion of the stirring, the composite was dried at 60°C for 5 h.

2.8.2. Thermal regeneration

1.0 g of the CTS/ZMS composite saturated with nitrate was placed in an oven and heated at 200°C for 24 h.

2.8.3. Chemical regeneration

1.0 g of the CTS/ZMS composite saturated with nitrate was placed in 100 mL solution containing HCl, NaOH, NaCl, Na₂CO₃, NaHCO₃, and CaCl₂, respectively, with the concentration of every chemical being 1 mol/L. After rotating at a speed of 130 rpm for 24 h at room temperature, the composite particles were rinsed with deionized water and dried at 60°C for 5 h.

2.8.4. Adsorption analysis of regeneration

Adsorption capacity (q_r , mg/g) [Eq. (1)], nitrate removal efficiency (R , %) (Eq. 2), and regeneration rate (R_r , %) was analyzed for each sample at 9°C ± 1°C. Regeneration rate (R_r , %) was calculated as described in Eq. (10):

$$R_r = \frac{q_{er}}{q_{en}} \times 100\% \quad (10)$$

where R_r is the regeneration rate (%), q_{er} is the equilibrium adsorption capacity of regenerated CTS/ZMS composite (mg/g), q_{en} is the equilibrium adsorption capacity of the fresh CTS/ZMS composite (mg/g). The analysis results of the tests were the average values of three replicates.

3. Results and discussion

3.1. Effect of adsorbent dose

In order to optimize the effect of adsorbent dose (Fig. 1), in 100 mL water solution of pH 7 ± 0.5 containing 30 mg/L of nitrate at 9°C ± 1°C, different doses of CTS/ZMS, that is 0.3, 0.5, 0.8, 1.0, 1.2, and 1.5 g/L were added and equilibrated for 420 min. The obtained results showed that when the adsorbent dose was increased from 0.3 to 1.0 g, the nitrate removal efficiency showed an increasing trend from 26.7% to 70.2% but thereafter further increase in dosage of CTS/ZMS to 1.5 g did not result in any increase in the removal efficiency of nitrate. Hence 1.0 g/100 mL is the optimum dose rate of CTS/ZMS.

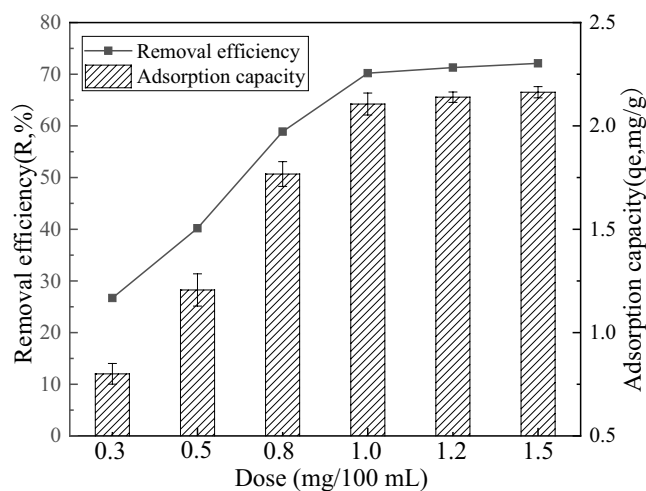


Fig. 1. Effect of adsorbent dose on nitrate removal.

3.2. Effect of contact time

Fig. 2 shows the effect of contact time on the nitrate adsorption capacities of the CTS/ZMS particles. Under the condition of the experiment, nitrate ion removal rate was increasing at faster rate with increasing contact time up to 180 min. When the reaction was carried out for 420 min, the adsorption capacity remained almost constant, indicating that the reaction had reached equilibrium and the optimal adsorption contact time was 420 min.

3.3. Effect of pH value

The results of the experiments on the effect of varying pH on the nitrate adsorption of CTS/ZMS are given in Fig. 3. As evident from Fig. 3, there is no significant change in the nitrate removal efficiency of CTS/ZMS (63.06%–71.3%) in the studied pH range of 4–10, indicating no significant effect of pH on the nitrate sorption capacity of CTS/ZMS. The point of zero charge for CTS/ZMS was obtained at pH 10.0 (Fig. 4). When the solution pH is higher than the point of zero charge, adsorbent surface becomes negatively charged, and as a result of electrostatic repulsion with the negatively charged nitrate ions, no adsorption of nitrate takes place [36]. The pH of test water being 7 ± 0.5, the CTS/ZMS composite have good adsorption capacity for nitrate under neutral conditions.

3.4. Effect of temperature

Temperature effect on the nitrate adsorption by CTS/ZMS is shown in Fig. 5. As evident from Fig. 5, increasing temperature led to increasing adsorption capacity as well as removal efficiency for nitrate. The adsorption capacity of CTS/ZMS for nitrate at 9°C ± 1°C was 2.11 mg/g which was increased to 2.23 mg/g at 20°C, with the corresponding removal rates being 70.2% and 74.5%, respectively. This result is different from that reported by Arora et al. [15] who studied the natural zeolite coated with chitosan (Ch-Z) to capture nitrate from water at 4°C and 20°C. In order to further study the effect of temperature, thermodynamic analysis was also conducted.

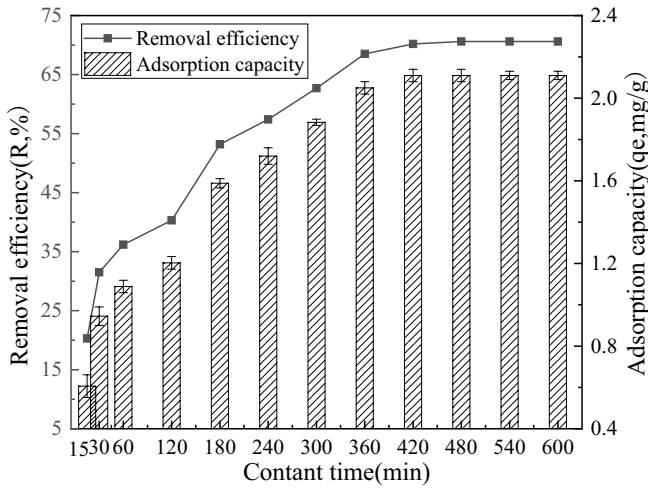


Fig. 2. Effect of contact time on nitrate removal.

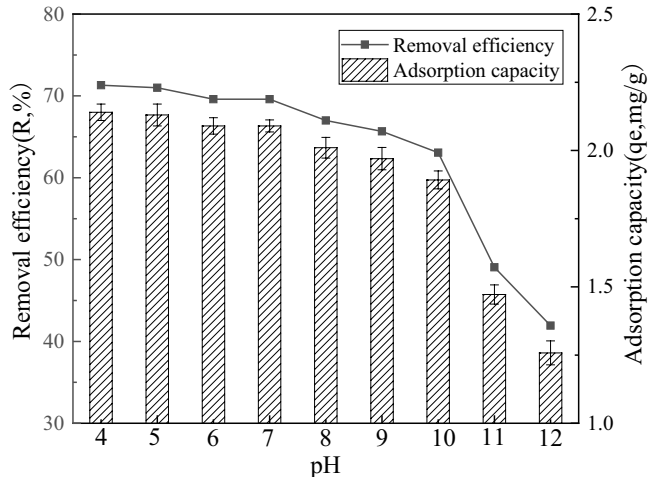


Fig. 3. Effect of pH value on adsorption of nitrate.

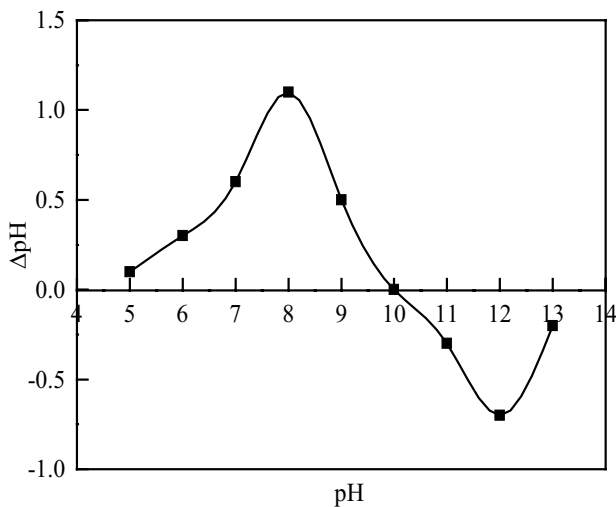


Fig. 4. Measurement curve of pH_{PZC} .

3.5. Thermodynamic studies

Thermodynamic parameters of adsorption such as standard free energy change (ΔG°), standard enthalpy change (ΔH°), and standard entropy change (ΔS°) were calculated from the experiments at varying temperatures. The values of ΔH° and ΔS° , calculated from the van't Hoff plot of $\ln K$ vs. $1/T$ (Fig. 6) are presented in Table 2.

Increase in the values of K with increasing temperature suggested that high temperature improved the adsorption of nitrates on the CTS/ZMS. The negative values of ΔG° for CTS/ZMS at all the temperatures confirmed that the adsorption of nitrate was spontaneous and thermodynamically favourable. The values of ΔS° for CTS/ZMS adsorbents was found to be 6.94×10^{-3} KJ/(K mol). This value indicated that there was increase in the randomness at the solid-liquid interface during adsorption of nitrates on the adsorbent [37]. The values of ΔH° for CTS/ZMS suggested that the adsorption of nitrate was endothermic, and this

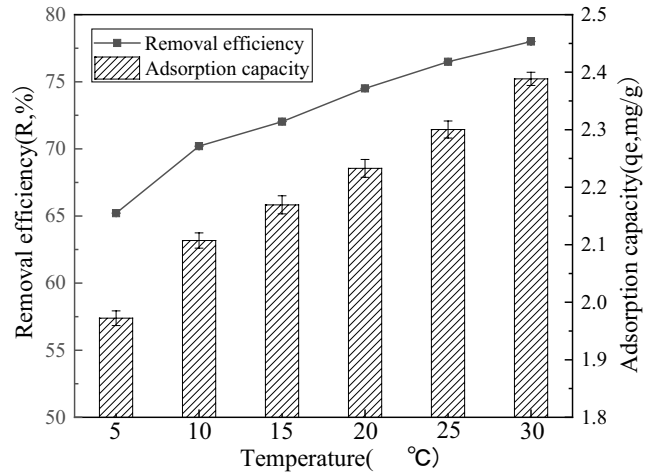


Fig. 5. Effect of temperature on nitrate removal.

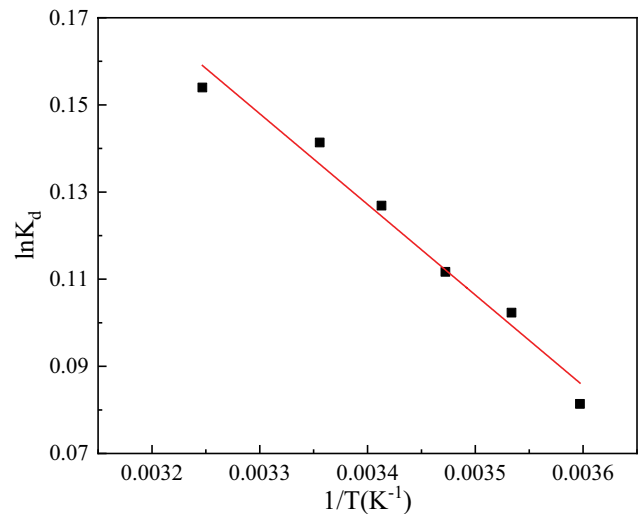


Fig. 6. Plot of $\ln K_d$ vs. $1/T$ for nitrate adsorption on CTS/ZMS.

Table 1

Comparative evaluation of adsorption capacity of some different adsorbents based on chitosan for nitrate removal

Materials	Initial nitrate concentration	pH	Dose	Temperature	Contact time	Adsorption capacity	Reference
Chitosan-zeolite (Ch-Z)	3,100 mg/L	–	0.4 g/250 mL	4°C	72 h	37.2 mg/g	[15]
	620 mg/L			20°C		45.8 mg/g	[15]
Chitosan-Fe(III)–Al(III)	150 mg/L	3	5 g/L	15°C	–	8.58 mg/g	[21]
Chitosan/Zeolite/nano ZrO ₂	20 mg/L	3	0.02 g/L	35°C	60 min	42.5%	[24]
Chitosan/polystyrene/zinc	10 mg/L	3	0.5 g/L	–	30 min	90%	[25]
Chitosan-PEG	10 mg/L	3	0.1 g/L	Room temperature		50.68 mg/g	[26]
Fe ₃ O ₄ /ZrO ₂ /chitosan	1–1,000 mg/L	3	–	–	–	89.3 mg/g	[27]
Ag-TiO ₂ /c-Al ₂ O ₃ /Chitosan	100 mg/L	11	0.5 g/L	–	5 min	74%	[28]

Table 2

Thermodynamic parameters for nitrate adsorption on the CTS/ZMS

T (K)	K	ΔG° (KJ/mol)	ΔH° (KJ/mol)	ΔS° [KJ/(K mol)]
278	0.1874	–0.1881		
283	0.2356	–0.2407		
288	0.2571	–0.2674	1.7296	6.94×10^{-3}
298	0.2922	–0.3091		
303	0.3255	–0.3503		

fact was supported by the increase in the adsorption with increasing temperature.

3.6. Adsorption isotherms

In order to understand the adsorption process of nitrate by CTS/ZMS, adsorption isotherm experimental results were treated with the Langmuir and Freundlich isotherm models. Effect of initial concentration of nitrate on the uptake capacity of CTS/ZMS is given in Fig. 7. When the nitrate concentration of the water sample was increased from 10 to 80 mg/L, adsorption of nitrate on the CTS/ZMS adsorbent was gradually increased at low temperature (9°C ± 1°C). The amount of adsorption, q_e , increased from 0.75 to 3.83 mg/g. It can be seen from Fig. 8 and Table 3 that the Langmuir adsorption isotherm model can better describe the adsorption behavior of nitrate by CTS/ZMS, and the adsorption process is single-layer. When the adsorption sites on the adsorbent were all saturated, the adsorption amount didn't increase. It is generally considered that when $0.1 < 1/n < 0.5$, adsorption is easy to proceed, and in the isothermal formula, $1/n = 0.492$, so the adsorption proceeds readily.

3.7. Adsorption kinetics

Kinetic experiments were conducted to determine the rate of the nitrate adsorption and the time required to reach equilibrium. The results from the time dependent nitrate sorption were treated with both the kinetic models (Fig. 9). Table 3 shows the kinetic parameters from both the models. By correlating the kinetic data with the above two rate models, it was found that the plot of t/q_t against time produced straight line ($R^2 = 0.989$), which was more correlated

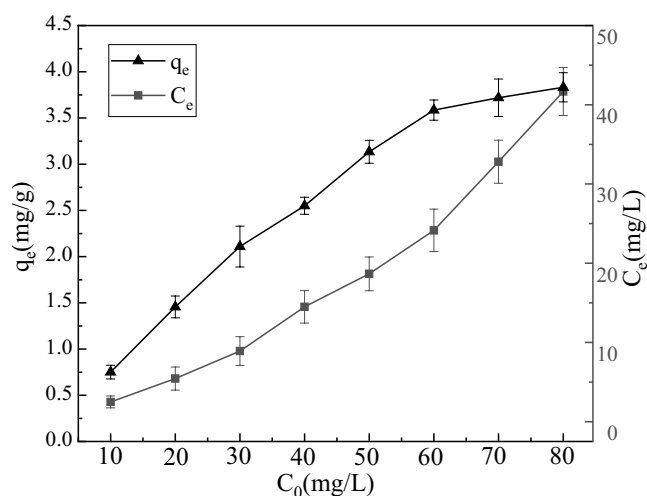


Fig. 7. Adsorption capacity for nitrate on CTS/ZMS: initial nitrate concentration from 10 to 80 mg/L.

than the pseudo-first-order model ($R^2 = 0.925$). The results showed that the adsorption process mainly followed the quasi-secondary rate model, and the whole process was controlled by chemical adsorption.

3.8. XRD analysis

Fig. 10 shows the XRD patterns of chitosan (CTS), ZMS, and CTS/ZMS composite. The peak of CTS at $2\theta = 11.8^\circ$ and 19.9° correspond to an amorphous structure of chitosan [38]. The diffraction peaks around 11° and 20° (2θ) observed for

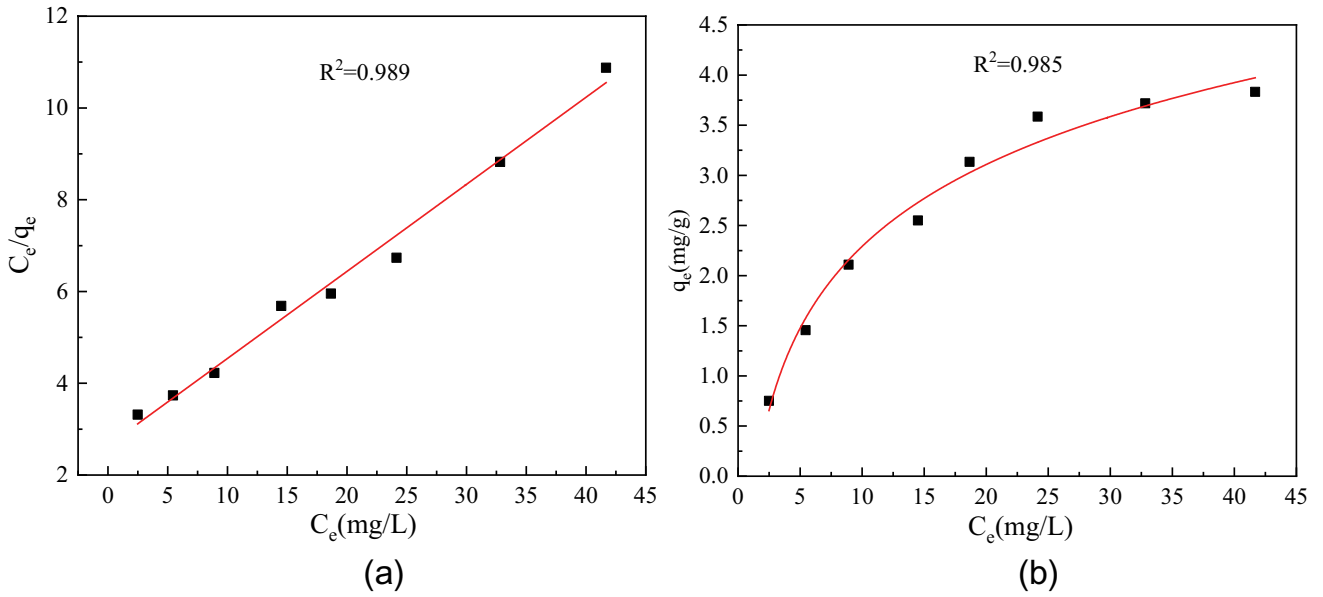


Fig. 8. (a) Langmuir and (b) Freundlich adsorption isotherm model.

Table 3
Parameters of kinetic, adsorption isotherm tests

Kinetic parameters						Adsorption isotherm parameters					
Quasi-first-order			Quasi-second-order			Langmuir			Freundlich		
q_e (mg/g)	k_1 (1/min)	R^2	q_e (mg/g)	k_2 (g/(mg min))	R^2	K_L (L/mg)	q_m (mg/g)	R^2	K_f (mg/g)/(mg/L) ^{1/n}	1/n	R^2
2.287	0.0099	0.925	2.382	0.006	0.989	0.072	5.271	0.989	2.291	0.492	0.985

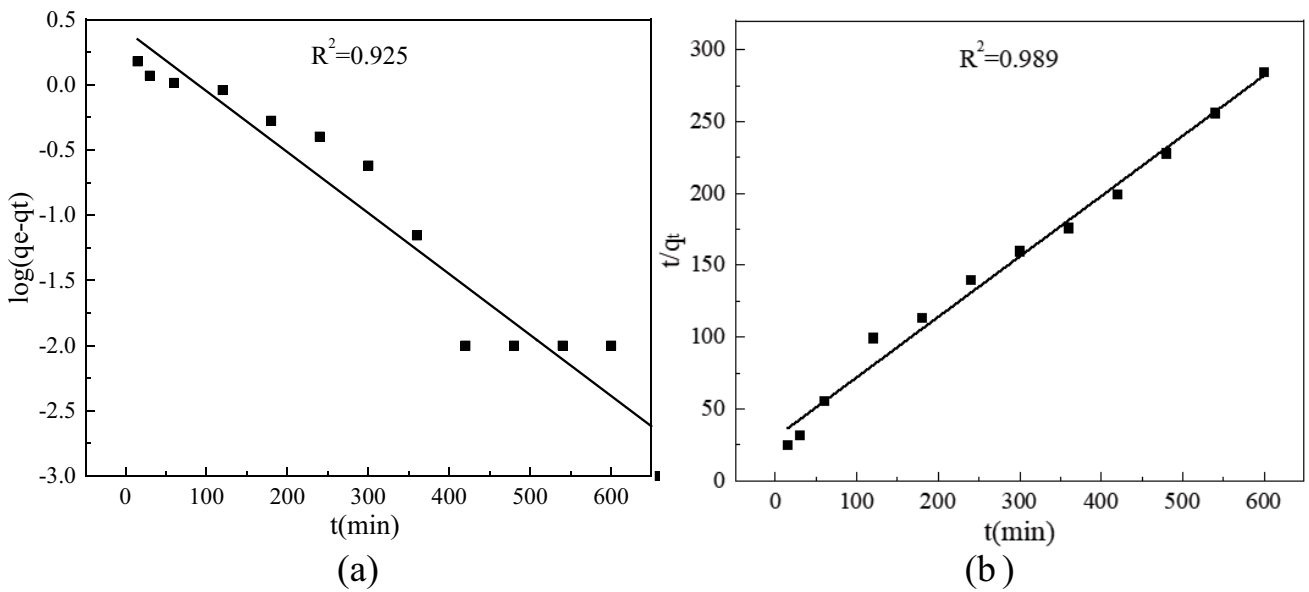


Fig. 9. Pseudo-first-order kinetic (a) and pseudo-second-order kinetic (b).

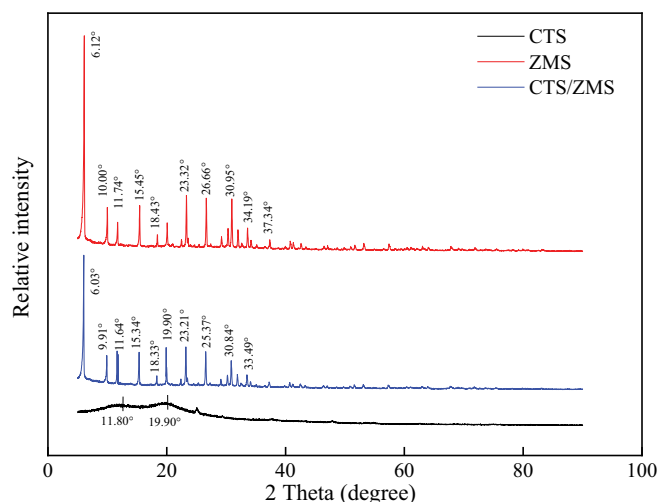


Fig. 10. XRD patterns of CTS, ZMS, and CTS/ZMS.

chitosan were in agreement with other published results [39]. From the characteristic peaks of ZMS, the 2θ values at 6.12° , 10.0° , 11.74° , 15.45° , 18.43° , 23.32° , 26.66° , 30.95° , 34.19° , and 37.34° had good agreement with the NaX zeolite crystal structure data file (JCPDS No. 38-0241) in the instrument library. The intensity of the peak at $2\theta = 19.9^\circ$ increased in the XRD of CTS/ZMS, suggesting that chitosan was intercalated into the ZMS. There were minor changes in the XRD patterns for CTS/ZMS and ZMS which indicated that the original ordered structure of ZMS was not destroyed by CTS [40].

3.9. FTIR analysis

FTIR spectra of the CTS, ZMS, and CTS/ZMS before and after nitrate adsorption in the scanning range of 4,000 to 400 cm^{-1} are shown in Fig. 11. In the spectrum of the chitosan (green line), the bands at $3,291$ and $1,591\text{ cm}^{-1}$ were attributed to the stretching vibrations of the $-\text{OH}$ group and $-\text{NH}_2$ group, respectively, which are the active groups of the chitosan [41]. In the spectrum of ZMS (black line), the band at $3,490\text{ cm}^{-1}$ was attributed to the tensile vibration of the $\text{Si}-\text{OH}$ group on the surface of the ZMS skeleton. The strong bands at 975 and 462 cm^{-1} were caused by $-\text{XO}_4$ and $\text{O}-\text{X}-\text{O}$ groups, respectively (X means Si/Al) [24]. These two bands indicated the basic tetrahedral skeleton of the ZMS. The FTIR spectra of the CTS/ZMS before adsorption (red line) of nitrate, showed a typical band at $1,654\text{ cm}^{-1}$ corresponding to the $\text{N}-\text{H}$ of the acetyl group. The band at $1,590\text{ cm}^{-1}$ was attributed to the stretching vibrations of the $-\text{NH}_2$ group [41]. The results showed that the functional groups of chitosan were loaded onto the surface of the ZMS. However, the stretching vibration of the $-\text{NH}_2$ group vanished after nitrate adsorption, the band at $1,376\text{ cm}^{-1}$ corresponding to the $\text{N}-\text{O}$ bond was observed in the spectrum of CTS/ZMS after the nitrate adsorption [42], which indicated that the group of $-\text{NH}_2$ was related to the nitrate adsorption. After the adsorption of NO_3^- , the $-\text{OH}$ vibration band changed from $3,490$ to $3,315\text{ cm}^{-1}$, which indicated that the $-\text{OH}$ group was also related to the nitrate adsorption. The bands

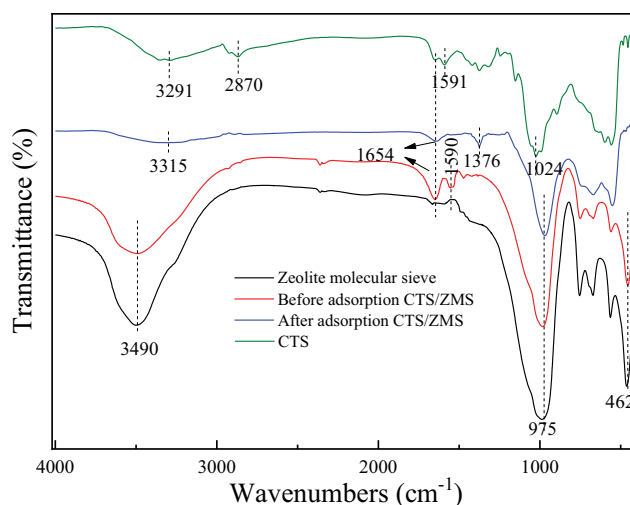


Fig. 11. FTIR spectrum of CTS, ZMS, and CTS/ZMS before and after nitrate adsorption.

of $-\text{XO}_4$ and $\text{O}-\text{X}-\text{O}$ group did not change before and after the adsorption of nitrate, indicating that the adsorption of nitrate did not change the basic structure of the CTS/ZMS.

3.10. XPS analysis

The adsorption mechanism of CTS/ZMS adsorption particles was studied by using XPS analysis of the composite before and after nitrate removal. The main peaks in the entire spectrum was observed at 75, 100, 300, 400, and 530 eV corresponding to the Al (2p), Si (2p), C (1s), N (1s), and O (1s), respectively. Except for the increase of peak intensity, there were no significant changes in the whole spectrum of the CTS/ZMS particles before and after nitrate adsorption (Fig. 12), which indicated that the adsorption of nitrate didn't affect the CTS/ZMS original structure, which was consistent with the FTIR analysis.

Binding energy of an element is related to its effective charge, different oxidation states. Existence of different electronic states of the O atoms can be analysed by the O (1s) binding energy. As shown in Figs. 13a and b, before nitrate adsorption, the binding energies corresponding to O (1s) were 531.5 and 531.3 eV which represented the $\text{X}-\text{OH}$ and $-\text{OH}$ groups, respectively. After nitrate adsorption by the CTS/ZMS composite, the binding energy of O (1s) were 531.7 and 531.4 eV with increase of 0.2 and 0.1 eV, respectively [43]. The increasing binding energy of O (1s) indicated that the density of electron clouds around the O atom decreased, which suggested the participation of the O-containing functional groups in the reaction with nitrate. When the $\text{X}-\text{OH}$ and $-\text{OH}$ groups participated in the reaction with nitrate ion, the binding energy of O (1s) increased [44].

The N (1s) spectra before nitrate adsorption exhibited two peaks at 402.74, and 399.5 eV corresponding to the $-\text{NHCO}$, and $-\text{NH}_2$ groups (Fig. 14a). After nitrate adsorption, new peak at 406.2 eV was observed, corresponding to the photoelectron peaks of $-\text{NO}_3^-$ (Fig. 14b). After nitrate adsorption, the peak at 399.5 eV corresponding to the $-\text{NH}_2$ group disappeared, and the peak of the $-\text{NH}_3^+$ group

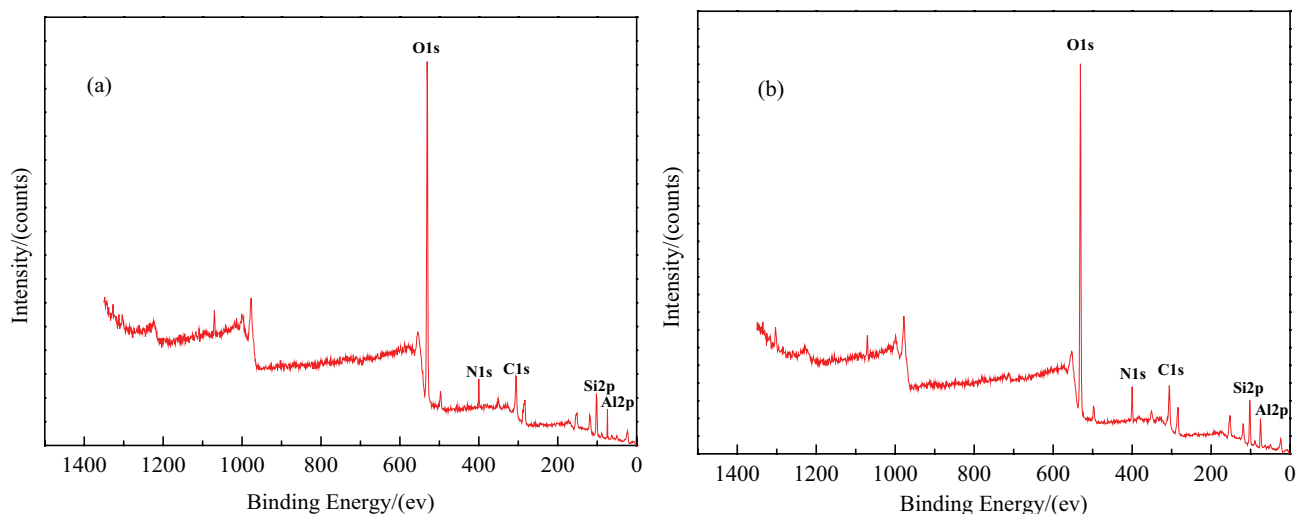


Fig. 12. Results of XPS spectrum of CTS/ZMS before (a) and after (b) nitrate adsorption.

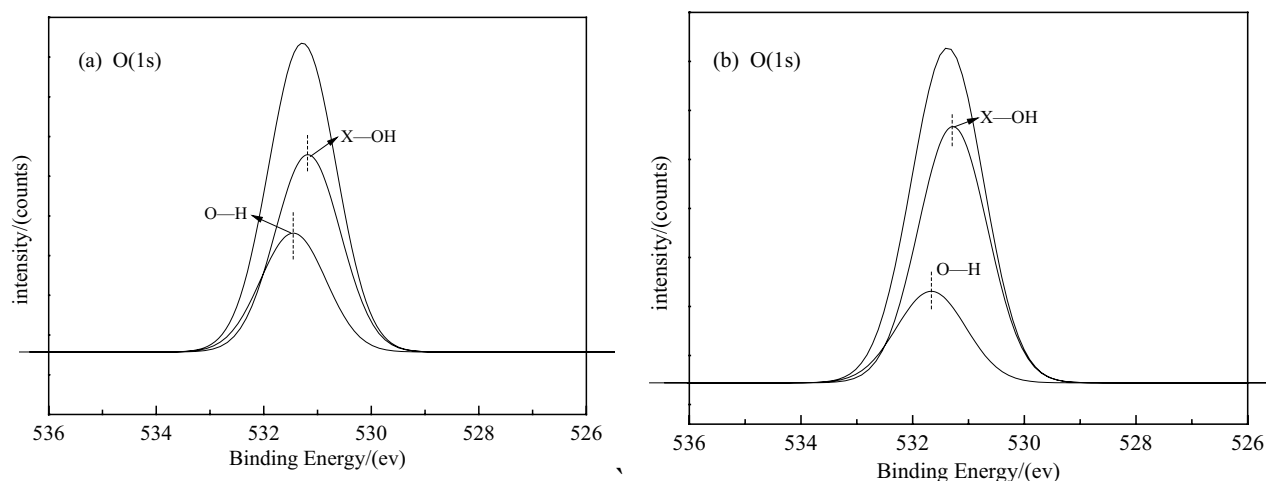


Fig. 13. Results of O (1s) spectrum of CTS/ZMS before (a) and after (b) adsorption.

appeared at 401.1 eV. It indicated that the $-\text{NH}_2$ group in the molecular structure of the CTS/ZMS changed to $-\text{NH}_3^+$ during the adsorption reaction, resulting in a change in the chemical environment of the N element. When $-\text{NH}_3^+$ was electrostatically bonded to the nitrate ion, it led to an increase in the binding energy of N (1s) [43,44], and the binding energy was 406.2 eV. The presence of nitrogen element in NO_3^- also indicated the electrostatic coupling of $-\text{NH}_3^+$ with the nitrate ions [44]. These results further validated the presence of nitrate adsorbed on the adsorbent, which was in accordance with the FTIR findings.

Fig. 15 shows the mechanism of nitrate adsorption by the CTS/ZMS. According to the results of FTIR and XPS, the removal of nitrate by CTS/ZMS was mainly through the electrostatic interaction between the $-\text{OH}$ and $-\text{NH}_2$ active groups and nitrate [24]. Previous studies on the effect of pH indicated that the point of zero charge was obtained at pH 10.0 (Fig. 4). When the solution pH value was lower

than the pH_{PZC} , the surface of the CTS/ZMS particles was positively charged (OH_2^+ , NH_3^+) [31]. Therefore, electrostatic reaction between NO_3^- and OH_2^+ , NH_3^+ present on the surface of CTS/ZMS [30,31] led to the adsorption of nitrate.

3.11. Regeneration studies

Good reusability and high adsorption capacity are very important for any adsorbent, which will significantly increase the economic value of the adsorption process [19]. The physical regeneration methods like water and heat regeneration were not efficient and stable due to long-time drying, and hence require higher costs. The chemical regeneration method has the advantages of high regeneration efficiency and low cost, and the adsorbent is often regenerated by using simple chemical reagents such as acid, alkali, and salt [45]. For CTS/ZMS composite, various regeneration methods like water regeneration, thermal

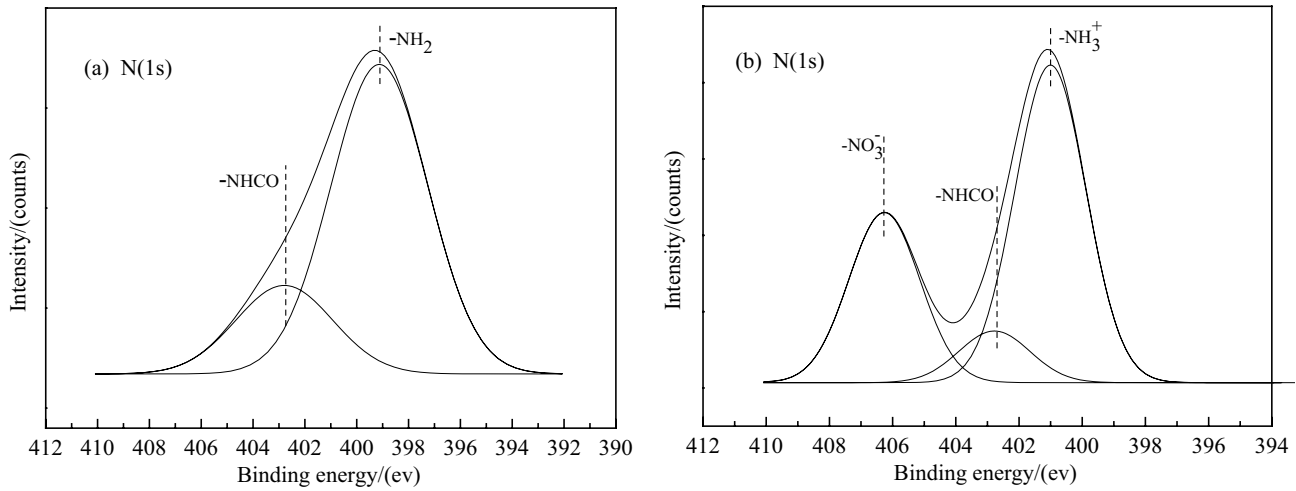


Fig. 14. Results of N(1s) spectrum of CTS/ZMS before (a) and after (b) adsorption.

regeneration, and chemical regeneration using NaHCO₃/Na₂CO₃/HCl/NaCl/CaCl₂/NaOH were studied as shown in Fig. 16a. It was evident that Na₂CO₃ solution could efficiently regenerate CTS/ZMS composite compared to other methods. Low price and good regeneration performance made Na₂CO₃ more economical for CTS/ZMS regeneration [46,47]. The adsorbed capacity of CTS/ZMS after Na₂CO₃ regeneration was 1.768 mg/g and regeneration rate was 83.7% when exposed to the nitrate solution of 30 mg/L concentration, at temperature of 9°C ± 1°C, dose of 1 g/100 mL, and contact time of 420 min. The adsorption particles regenerated by HCl (25.33%), NaCl (11.33%), and NaOH (2.0%)

solutions had relatively low removal rate of nitrate, due to the irreversible damage on the adsorption sites of CTS/ZMS caused by Cl⁻ and OH⁻, thus resulting in adverse effects on the adsorption of nitrate [48]. The regenerated adsorbent was used for five cycles after being regenerated by Na₂CO₃ solution after each sorption experiment. A comparison of the regeneration efficiency and adsorption capacity in five sequential runs is shown in Fig. 16b. After five runs, the adsorption capacity of the CTS/ZMS was 1.534 mg/g and regeneration rate was 70.4% (Fig. 16b). This proved that the adsorbent could be reused several times without any considerable loss of adsorption ability.

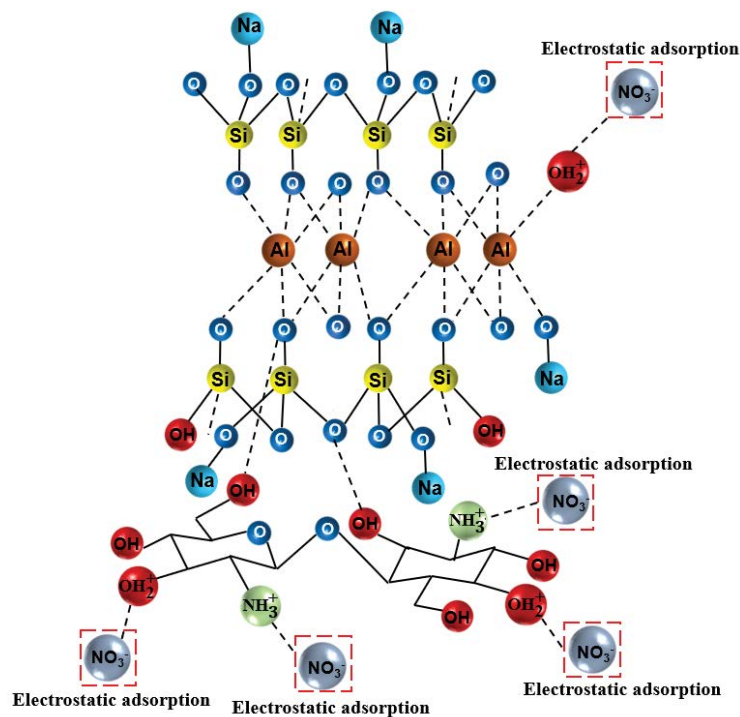


Fig. 15. Adsorption mechanism of CTS/ZMS and nitrate.

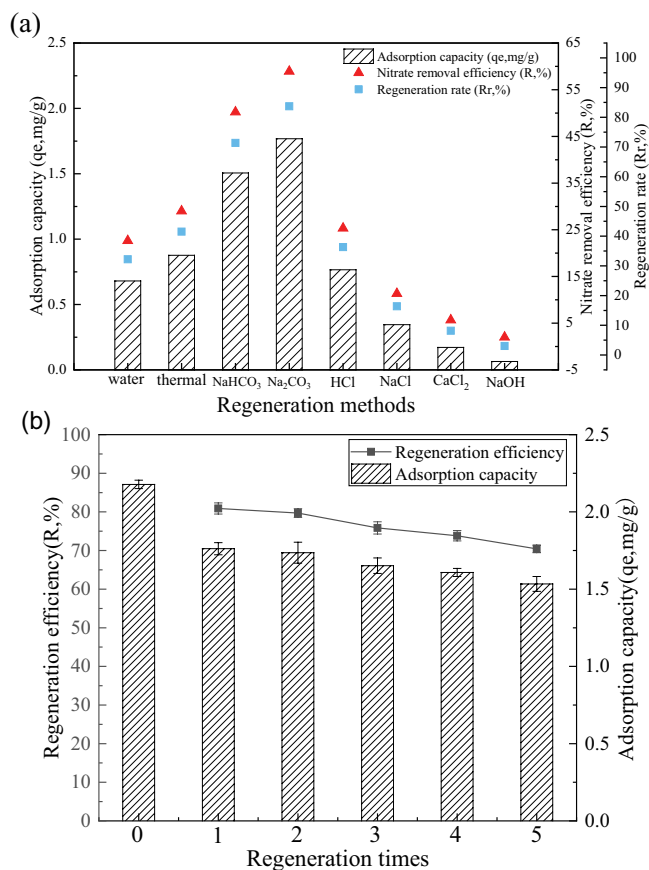


Fig. 16. Reuse studies for CTS/ZMS (a) different regenerants and (b) regeneration times.

4. Conclusions

In this research, a novel low-cost adsorbent, CTS/ZMS adsorbent was prepared by using environmental friendly chitosan (CTS) and ZMS. At temperature of $9^{\circ}\text{C} \pm 1^{\circ}\text{C}$ and pH value of 7.0, the optimal dosage and contact time for CTS/ZMS adsorbent were 1.0 g/100 mL and 420 min, respectively. FTIR, XPS studies showed that $-\text{NH}_2$ and $-\text{OH}$ groups participated in the electrostatic attraction between the adsorbent and nitrate. The adsorption isotherm and kinetics followed the Langmuir isotherm model and the pseudo-second-order model, respectively. Thermodynamic studies showed the adsorption of nitrate was spontaneous and endothermic. The CTS/ZMS composites can be reused at least five times when 1 mol/L Na_2CO_3 solution was used as a regenerant. The results obtained in this study illustrated that CTS/ZMS composite was a promising material for nitrate removal from low temperature groundwater. In the future, large scale implementation of this adsorbent needs to be developed. Also, further study should focus on optimizing the regeneration process and waste treatment of chemical regenerants.

Acknowledgment

This work was financially supported by National Natural Science Fund (51508342).

References

- [1] S. Ghafari, M. Hasan, M.K. Aroua, Bio-electrochemical removal of nitrate from water and wastewater – a review, *Bioresour. Technol.*, 99 (2008) 3965–3974.
- [2] Ministry of Environmental Protection of the People's Republic of China, 2018 China Environmental Status Bulletin, Beijing, 2018 (in Chinese).
- [3] L. Fewtrell, Drinking-water nitrate, methemoglobinemia, and global burden of disease: a discussion, *Environ. Health Perspect.*, 112 (2004) 1371–1374.
- [4] A. Sowmya, S. Meenakshi, An efficient and regenerable quaternary amine modified chitosan beads for the removal of nitrate and phosphate anions, *J. Environ. Chem. Eng.*, 1 (2013) 906–915.
- [5] National Health Commission of the People's Republic of China, Standard of Drinking Water Quality, Beijing, 2016 (in Chinese).
- [6] L. Zheng, T. Liu, Q. Yuan, Improvement measures of micro-polluted source water treatment process based on conventional treatment, *J. Environ. Manage. Coll. China*, 24 (2014) 61–64 (in Chinese).
- [7] T. He, Q. Ye, Q. Sun, X. Cai, J. Ni, Z. Li, D. Xie, Removal of nitrate in simulated water at low temperature by a novel psychrotrophic and aerobic bacterium, *Pseudomonas taiwanensis* strain, *J. Biomed. Res. Int.*, 2018 (2018) 1–9.
- [8] M. Alikhani, M.R. Moghbeli, Ion-exchange polyHIPE type membrane for removal nitrate ions: preparation, characterization, kinetics and adsorption studies, *Chem. Eng. J.*, 239 (2014) 93–104.
- [9] J. Chung, K. Amin, S. Kim, S. Yoon, K. Kwon, W. Bae, Autotrophic denitrification of nitrate and nitrite using thiosulfate as an electron donor, *Water Res.*, 58 (2014) 169–178.
- [10] W. Xing, D. Li, J. Li, Q. Hu, S. Deng, Nitrate removal and microbial analysis by combined micro-electrolysis and autotrophic denitrification, *Bioresour. Technol.*, 211 (2016) 240–247.
- [11] T. Wang, J. Lin, Z. Chen, M. Megharaj, R. Naidu, Green synthesized iron nano particles by green tea and eucalyptus leaves extracts used for removal of nitrate in aqueous solution, *J. Cleaner Prod.*, 83 (2014) 413–419.
- [12] L.A. Richards, M. Vuachère, A.I. Schäfer, Impact of pH on the removal of fluoride, nitrate and boron by nanofiltration/reverse osmosis, *Desalination*, 261 (2010) 331–337.
- [13] N.B. Singh, G. Nagpal, S. Agrawal, Rachna, Water purification by using adsorbents: a review, *Environ. Technol. Innovation*, 11 (2018) 187–240.
- [14] A. Bhatnagar, M. Sillanpää, A review of emerging adsorbents for nitrate removal from water, *Chem. Eng. J.*, 168 (2011) 493–504.
- [15] M. Arora, N.K. Eddy, K.A. Mumford, Surface modification of natural zeolite by chitosan and its use for nitrate removal in cold regions, *Cold Reg. Sci. Technol.*, 62 (2010) 92–97.
- [16] D. Bhardwaj, M. Sharma, P. Sharma, R. Tomar, Synthesis and surfactant modification of clinoptilolite and montmorillonite for the removal of nitrate and preparation of slow release nitrogen fertilizer, *J. Hazard. Mater.*, 227–228 (2012) 292–300.
- [17] S. Tyagi, D. Rawtani, N. Khatri, M. Tharmavaram, Strategies for nitrate removal from aqueous environment using nanotechnology: a review, *J. Water Process Eng.*, 21 (2018) 84–95.
- [18] R. Wu, Q. Ye, K. Wu, S. Cheng, T. Kang, H. Dai, Adsorption performance of CMK-3 and C-FDU-15 in NO removal at low temperature, *J. Environ. Sci.*, 87 (2020) 289–298.
- [19] Q. Hu, N. Chen, C. Feng, W. Hu, Nitrate adsorption from aqueous solution using granular chitosan- Fe^{3+} complex, *Appl. Surf. Sci.*, 34 (2015) 1–9.
- [20] J. Wang, C. Chen, Chitosan-based biosorbents: modification and application for biosorption of heavy metals and radionuclides, *Bioresour. Technol.*, 60 (2014) 129–141.
- [21] Q. Hu, N. Chen, C. Feng, W. Hu, J. Zhang, H. Liu, Q. He, Nitrate removal from aqueous solution using granular chitosan- Fe(III)-Al(III) complex: kinetic, isotherm and regeneration studies, *J. Taiwan Inst. Chem. Eng.*, 63 (2016) 216–225.
- [22] P.B. Gustavo, S.D. Henrique, S. Patrícia, B.S. Eliana, F.S. Cláudio, Design and characterization of chitosan/zeolite composite

- films-Effect of zeolite type and zeolite dose on the film properties, *Mater. Sci. Eng., C*, 60 (2016) 246–254.
- [23] X. Liu, R. Wang, Effective removal of hydrogen sulfide using 4A molecular sieve zeolite synthesized from attapulgite, *J. Hazard. Mater.*, 326 (2017) 157–164.
- [24] A. Teimouri, S.G. Nasab, N. Vahdatpoor, S. Habibollahi, H. Salavati, A.N. Chermahini, Chitosan/zeolite Y/nano ZrO₂ nanocomposite as an adsorbent for the removal of nitrate from the aqueous solution, *Int. J. Biol. Macromol.*, 93 (2016) 254–266.
- [25] M. Keshvardoostchokami, S. Babaei, F. Piri, A. Zamani, Nitrate removal from aqueous solutions by ZnO nanoparticles and chitosan-polystyrene-Zn nanocomposite: kinetic, isotherm, batch and fixed-bed studies, *Int. J. Biol. Macromol.*, 101 (2017) 922–930.
- [26] A. Rajeswari, A. Amalraj, A. Pius, Adsorption studies for the removal of nitrate using chitosan/PEG and chitosan/PVA polymer composites, *J. Water Process Eng.*, 9 (2016) 123–134.
- [27] H. Jiang, P. Chen, S. Luo, X. Tu, Q. Cao, M. Shu, Synthesis of novel nanocomposite Fe₃O₄/ZrO₂/chitosan and its application for removal of nitrate and phosphate, *Appl. Surf. Sci.*, 284 (2013) 942–949.
- [28] S. Zarei, N. Farhadian, R. Akbarzadeh, M. Pirsaeheb, A. Asadi, Z. Safaei, Fabrication of novel 2D Ag-TiO₂/c-Al₂O₃/chitosan nano-composite photocatalyst toward enhanced photocatalytic reduction of nitrate, *Int. J. Biol. Macromol.*, 145 (2020) 926–935.
- [29] Y. Gao, Y. Ru, L. Zhou, Preparation and characterization of chitosan-zeolite molecular sieve composite for ammonia and nitrate removal, *Adv. Compos. Lett.*, 27 (2018) 185–192.
- [30] P. Chutia, S. Kato, T. Kojima, S. Satokawa, Arsenic adsorption from aqueous solution on synthetic zeolites, *J. Hazard. Mater.*, 162 (2009) 440–447.
- [31] S.K. Milonjić, A consideration of the correct calculation of thermodynamic parameters of adsorption, *J. Serb. Chem. Soc.*, 72 (2007) 1363–1367.
- [32] I. Langmuir, The adsorption of gases on plane surfaces of glass, mica and platinum, *J. Am. Chem. Soc.*, 40 (1918) 1361–1403.
- [33] H. Freundlich, Über die adsorption in Lösungen, *Z. Phys. Chem.*, 57 (1906) 1996–2001.
- [34] S. Lagergren, About the theory of so-called adsorption of solution substances, *Kung. Sven. Vetén. Hand.*, 24 (1989) 1–39.
- [35] J. Kong, Q. Yue, S. Sun, B. Gao, Y. Kan, Q. Li, Y. Wang, Adsorption of Pb(II) from aqueous solution using keratin waste – hide waste: equilibrium, kinetic and thermodynamic modeling studies, *Chem. Eng. J.*, 241 (2014) 393–400.
- [36] Y. Xie, S. Li, G. Liu, J. Wang, K. Wu, Equilibrium, kinetic and thermodynamic studies on perchlorate adsorption by cross-linked quaternary chitosan, *Chem. Eng. J.*, 192 (2012) 269–275.
- [37] M. Kara, H. Yuzer, E. Sabah, M.S. Celik, Adsorption of cobalt from aqueous solutions onto sepiolite, *Water Res.*, 37 (2003) 224–232.
- [38] J.W. Rhim, S.I. Hong, H.M. Park, P.K.W. Ng, Preparation and characterization of chitosan-based nanocomposite films with antimicrobial activity, *J. Agric. Food. Chem.*, 54 (2006) 5814–5822.
- [39] B.W.S. Souza, M.A. Cerqueira, J.T. Martins, A. Casariego, J.A. Teixeira, A.A. Vicente, Influence of electric fields on the structure of chitosan edible coatings, *Food Hydrocolloids*, 24 (2010) 330–335.
- [40] W. Thakhiew, S. Devahastin, S. Soponronnarit, Physical and mechanical properties of chitosan films as affected by drying methods and addition of antimicrobial agent, *J. Food Eng.*, 119 (2013) 140–149.
- [41] M. Islam, R. Patel, Nitrate sorption by thermally activated Mg/Al chloride hydrotalcite-like compound, *J. Hazard. Mater.*, 169 (2009) 524–531.
- [42] I. Mobasherpour, S. Heshajin, M. Kazemzadeh, M. Zakeri, Synthesis of nanocrystalline hydroxyapatite by using precipitation method, *J. Alloys Compd.*, 430 (2007) 330–333.
- [43] C. Fan, H. Ma, L. Hua, FTIR and XPS analysis of characteristics of synthesized zeolite and removal mechanisms for Cr(III), *Spectrosc. Spectr. Anal.*, 32 (2012) 324–329 (in Chinese).
- [44] R. Ramya, P.N. Sudha, J. Mahalakshmi, Preparation and characterization of chitosan binary blend, *Int. J. Sci. Res. Publ.*, 2 (2012) 2250–3153.
- [45] J. Chen, X. Wang, S. Zhou, Z. Chen, Effect of alkalinity on bio-zeolite regeneration in treating cold low-strength ammonium wastewater via adsorption and enhanced regeneration, *Environ. Sci. Pollut. Res.*, 26 (2019) 28040–28052.
- [46] E. Gabruś, K. Witkiewicz, J. Nastaj, Modeling of regeneration stage of 3A and 4A zeolite molecular sieves in TSA process used for dewatering of aliphatic alcohols, *Chem. Eng. J.*, 337 (2018) 416–427.
- [47] M. Islam, R. Patel, Physicochemical characterization and adsorption behavior of Ca/Al chloride hydrotalcite-like compound towards removal of nitrate, *J. Hazard. Mater.*, 190 (2011) 659–668.
- [48] W. Zhang, Z. Zhou, Y. An, S. Du, D. Ruan, C. Zhao, X. Ren, Optimization for zeolite regeneration and nitrogen removal performance of a hypochlorite-chloride regenerant, *Chemosphere*, 178 (2017) 565–572.